Citation: Pratama, W., S. Kita (2022), Stress field orientation obtained from earthquake focal mechanisms in Indonesia region, Synopsis of IISEE-GRIPS Master's Thesis.

STRESS FIELD ORIENTATION OBTAINED FROM EARTHQUAKE FOCAL MECHANISMS IN INDONESIA REGION

Wahyudi Nasrul Pratama[1] **Supervisor: Saeko KITA**[2]
MEE21706

ABSTRACT

Determination of the stress field is essential to understanding the stress source and earthquake mechanism. However, the stress field study has been rarely conducted in the Indonesia region. We constructed the stress map in Indonesia derived from the Global Centroid Moment Tensor (GCMT) and the National Research Institute for Earth Science and Disaster Prevention (NIED) focal mechanism data from 1990 until 2021, where the Agency for Meteorology, Climatology, and Geophysics, Indonesia (BMKG)'s stations were also used for determining focal mechanisms in the NIED catalog. Overall, we used 3,756 earthquake focal mechanism data with a depth of $\leq$30 km. We applied two methodologies in this study; firstly, we created a mesh size of 75 km x 75 km of spatial mean of maximum horizontal compression stress (SHmax) and fault type. Then, we also performed the stress tensor inversion method to confirm the spatial mean of SHmax orientations. We got very declivous plunges of σ_1 in the northern North Maluku, southern North Maluku, and Batu-Mentawai-Pagai subduction segments. Meanwhile, the West and Central Java, the East Java, and the Sumba subduction segments have relatively steeper plunge angles than other regions. We found that the two methodologies we used yielded the same results in general. In our stress map, the orientations of SHmax are commonly perpendicular to the trench in the subduction zone and subparallel to the plate motion. This stress map also revealed the fault type distribution, which is generally consistent with the tectonic setting and focal mechanisms of large earthquakes. We confirmed that the normal faulting associated with SHmax parallel to the trench is intense near the trench of Java and Sumba subduction segments, indicating this area as the uncouple subduction zone. Stress field map in this study has possibility to assess the potential slip of faults in Indonesia for future prospects.

Keywords: Stress Map, Stress Tensor Inversion, SHmax, Focal Mechanisms.

1. INTRODUCTION

Examination of stress fields is essential for providing knowledge about stress sources and earthquake mechanics. Several kinds of stress field studies have been conducted in some regions of Indonesia. However, those studies just examined stress field in limited areas, mostly the western part of Indonesia, and just a little information about stress fields in the eastern part of Indonesia. Aiming to fill the gap, this study intends to present the stress orientation in entire Indonesia region. We used earthquake data catalogs to get the stress orientation because there are many focal mechanism data provided by the Global Centroid Moment Tensor (GCMT) (Dziewonski et al., 1981; Ekström et al., 2021) and the source-parameter determinations based on waveform inversion of the Fourier Transformed seismograms (SWIFT) system developed by the National Research Institute for Earth Science and Disaster Prevention (NIED), where the Agency for Meteorology, Climatology, and Geophysics, Indonesia (BMKG)'s stations were also used for determining focal mechanisms in the NIED catalog (Nakano et al. 2010; Inazu et al. 2016).

[1] Agency for Meteorology, Climatology and Geophysics, Republic of Indonesia.
[2] International Institute of Seismology and Earthquake Engineering, Building Research Institute.

2. DATA

We compiled GCMT focal mechanism data from International Seismological Centre (ISC) (Lentas, 2017; Lentas et al., 2019) and the SWIFT system by NIED in this study with the following criteria: We only used shallow earthquake (≤30 km depth) data to represent the crustal stress with a period from 1990 to 2021 for magnitude (Mw) of 4.3 to 9.0 earthquakes. Focal mechanism data in GCMT were adopted from 1990 to July of 2007 in our compilation data, because NIED data starts from the middle of 2007. After that period, we combined both catalogs to increase the number of focal mechanisms for data processing. We considered NIED data as the primary fault orientation because they also used seismic waveforms from the Indonesia broadband seismograph network by BMKG. In addition, the source centroid locations were more consistent with the hypocenter determination of USGS compared to GCMT (Nakano et al., 2010). In total, we used 3,756 events (2,362 events from GCMT and 1,394 events from NIED) in this study. Then, before inverting the focal mechanisms, we grouped them into smaller areas (Figure 1). In the subduction zone, we used segmentations of the subduction zone in Indonesia from Irsyam et al. (2017) with some modifications. Besides that, we classified the other regions using events which have close epicenter distribution and similar focal mechanisms in the majority.

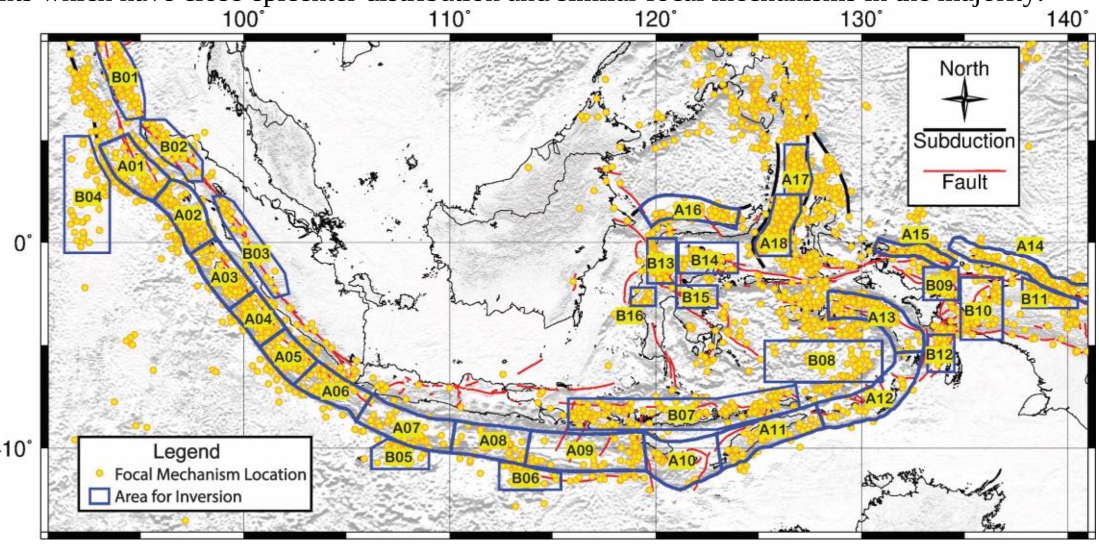

Figure 1. Distribution of compiled focal mechanism data (yellow dots) and area for stress inversions. Segmentation of subduction zone based on Irsyam et al. (2017) with some modifications.

3. METHODOLOGY

In order to examine the spatial pattern of stress orientation, we adopted a methodology by Imanishi et al. (2019). However, this methodology determines the stress field orientation by calculating the circular mean of SHmax derived from focal mechanism P, B, and T axes in each grid. Therefore, the quality is not better than the stress inversion result (Heidbach et al., 2010). However, the advantage of this method is that the spatial distribution of the stress field can be obtained to analyze the heterogeneity of the stress field in the study area. Therefore, to fulfill the lack of this method, we also performed the stress tensor inversions in 34 areas in the Indonesian archipelago, using a code by Vavryčuk (2014) as a confirmation.

We adopted Imanishi et al. (2019) methodology to construct a spatial stress mapping for this study. Firstly, P, T, and B axes from individual earthquake focal mechanisms were converted to SHmax orientation using Zoback (1992) classification. The methodology by Imanishi et al. (2019) also provides information of the fault type, using a method of Shearer et al. (2006) based on rake angles of focal mechanisms. Then, we used a 75 km x 75 km mesh considering the amount of data. The stress field map was constructed using the procedure as follows: (1) take earthquakes within a radius of 100 km around the mesh, (2) if the number of earthquakes in a mesh was equal to or larger than 5, calculate the weighted average of the SHmax and the fault type value. The weight of each earthquake depends on the distance from a mesh following Allmendinger et al. (2007), in which we chose α equal to 50. Then, we used circular statistics for calculating the weighted mean and standard deviation of SHmax at each mesh (Mardia, 1972).

We converted the stress orientation from inversion method to SHmax, where the orientation of SHmax is better to be used than principal stress direction for displaying tectonic stress results to avoid an error if the principal stress direction is used. SHmax can be calculated from four stress tensor inversion parameter results using a procedure by Lund and Townend (2007).

4. RESULTS AND DISCUSSION

The spatial mean of the SHmax and fault type was created using a mesh size of 75 km in both longitude and latitude directions (Figure 2a). The SHmax orientations are indicated by the straight line and its fault types are indicated by the background color. Generally, the stress field is perpendicular to the trench axis in the subduction zone with dominant thrust faulting. In the Java region, the focal mechanism data were not so much compared to the subduction region, so the spatial mean of SHmax and fault type was not too dense. Then, in this region, stress field orientations near the subduction zone were dominantly parallel to the trench axis associated with normal faulting. This condition also happened in Aru Island, the south of Bird's Head Region Papua. We also generated the deviation of mean SHmax and fault type for each mesh (Figures 2b and 2c). In majority, the mean of SHmax standard deviation was less than 40^o. The higher standard deviation of SHmax indicated a non-uniformity stress field in that region. The higher standard deviation for the fault type means that more fault type heterogeneity happened at the mesh, which is indicated by yellow to red in Figure 2c.

In case of stress tensor inversion, overall, we used enough data for conducting the stress inversions in the subduction segments (A areas), except in the West Nusa Tenggara subduction segment (A10), in which only 14 pieces of focal mechanism data were available. The σ_1 azimuths for each subduction segment are nearly perpendicular to the trenches, with opposite directions of the subduction dip, and the azimuths vary for each subduction segment. The plunge angles of σ_1 for each subduction segment vary in the range of 3.36^o – 58.68^o. The northern North Maluku (A17), the southern North Maluku (A18), and the Batu-Mentawai-Pagai (A03) subduction segments have very declivous plunges with 3.39^o, 6.68^o, and 7.68^o, respectively. Meanwhile, the West and Central Java (A07), the East Java (A08), and the Sumba (A09) subduction segments have relatively steeper plunge angles with 49.56^o, 58.68^o, and 50.73^o, respectively. For the stress ratio R in the subduction zones, all segments produce the stress ratio R close to 1, which indicates compressional stress which is dominant in this area. Then, based on the misfit angles, all segments yield angle less than 45^o, indicating the valid result of the inversion. The largest misfit angle occurred in the South Banda subduction segment (A12), with a misfit angle equal to 31.76^o.

On the other hand, in the non-subduction segment (B areas), we conducted stress inversions in 16 areas (B01 – B16). The minimum number of data that we used for these areas is 20 pieces of focal mechanism data, namely in the Mamuju fault (B16). The values of stress ratio R vary in B areas. Dominant extensional stress occurred in several regions, namely the Andaman Sea fault (B01), the Sumatera outer-rise (B04), the West-Central Java outer-rise (B05), the East Java outer-rise (B06), the Aru trough (B12), the Palu-Koro fault (B12), and the Batui-Balantak fault (B14). In contrast, in the other B areas compressional stress is dominant. All inversion results showed the valid results according to the misfit angle. The misfit angle for B areas is in the range of 11.51^o – 36.42^o, with the largest misfit in the Batui-Balantak fault (B14). We calculated and plotted the azimuth of SHmax from 4 parameters inversion results based on a mathematical approach of Lund and Townend (2007) (Figure 3a).

In order to confirm those results, we plotted the SHmax azimuths from the methodology of Imanishi et al. (2019) and SHmax inferred from stress inversions into a map. The small colored rectangle indicates the spatial SHmax, the colored one indicates the stress regime (normal, strike-slip and thrust fault) in that area, and the long black bars show the SHmax which is derived from the inversions. In general, those methods reveal the same stress orientation. It must note that the stress orientations from inversion are the regional stress according to inversion area.

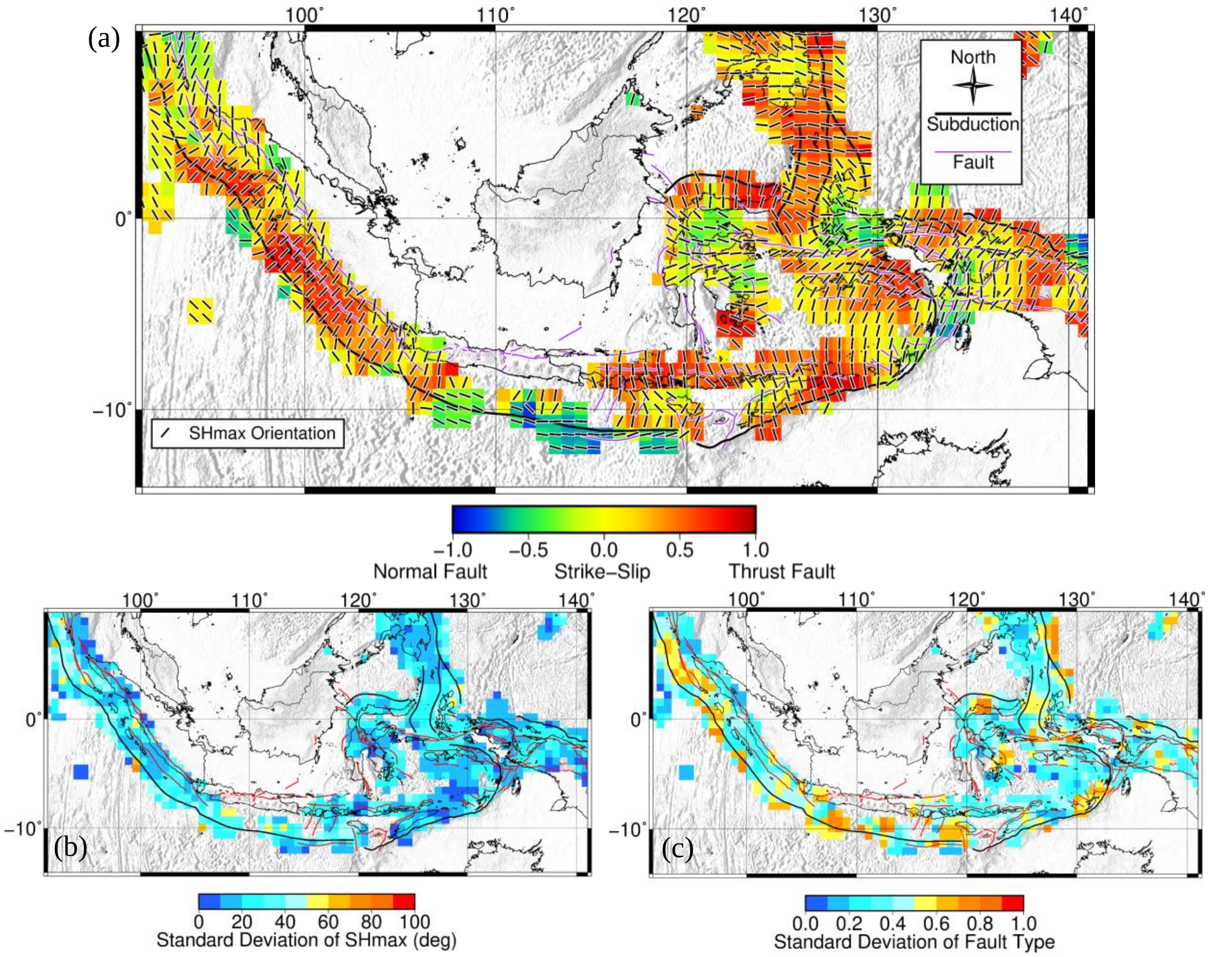

Figure 2. (a) Spatial mean of SHmax orientation and fault type using a mesh size of 75 km x 75 km. (b) Standard deviation of the mean SHmax. (c) Standard deviation of the mean fault type.

We confirmed that the normal faulting associated with SHmax parallel to the trench is intense near the trench of Java and Sumba subduction segments, indicating this area as the uncouple subduction zone (Christensen and Ruff, 1988). This condition is supported by stress tensor inversions that revealed radial to pure extensive tectonic stress regime in these regions. We also compared the spatial mean fault type map with earthquakes M≥7. The result revealed that our stress map is generally consistent with focal mechanisms of these large events. It means that the focal mechanisms of future large earthquakes will be also consistent with this stress map. The most striking discrepancy in focal mechanism occurred in the Java region, where the thrusting mechanism in 1994 and 2006 Java earthquakes lie in the strike-slip to normal fault region in our map, these are unusual cases because it is difficult to create thrust faulting event in the uncouple subduction zone like those in Java region (Bilek and Engdahl, 2007).

5. CONCLUSIONS

This study has created the stress map for the entire Indonesia derived from the GCMT and NIED focal mechanism data, filling the gap in the stress field from previous studies. The two methodologies we applied in this study revealed a good agreement with each other in the SHmax orientation. Overall, the SHmax directions are perpendicular to the trench in the subduction zone and subparallel with plate motion, except in the Java subduction zone, which is dominated by the parallel SHmax orientations to the trench. In this stress map, we also added information on the spatial mean of fault types which is generally consistent with the tectonic setting and focal mechanism of large earthquakes in Indonesia.

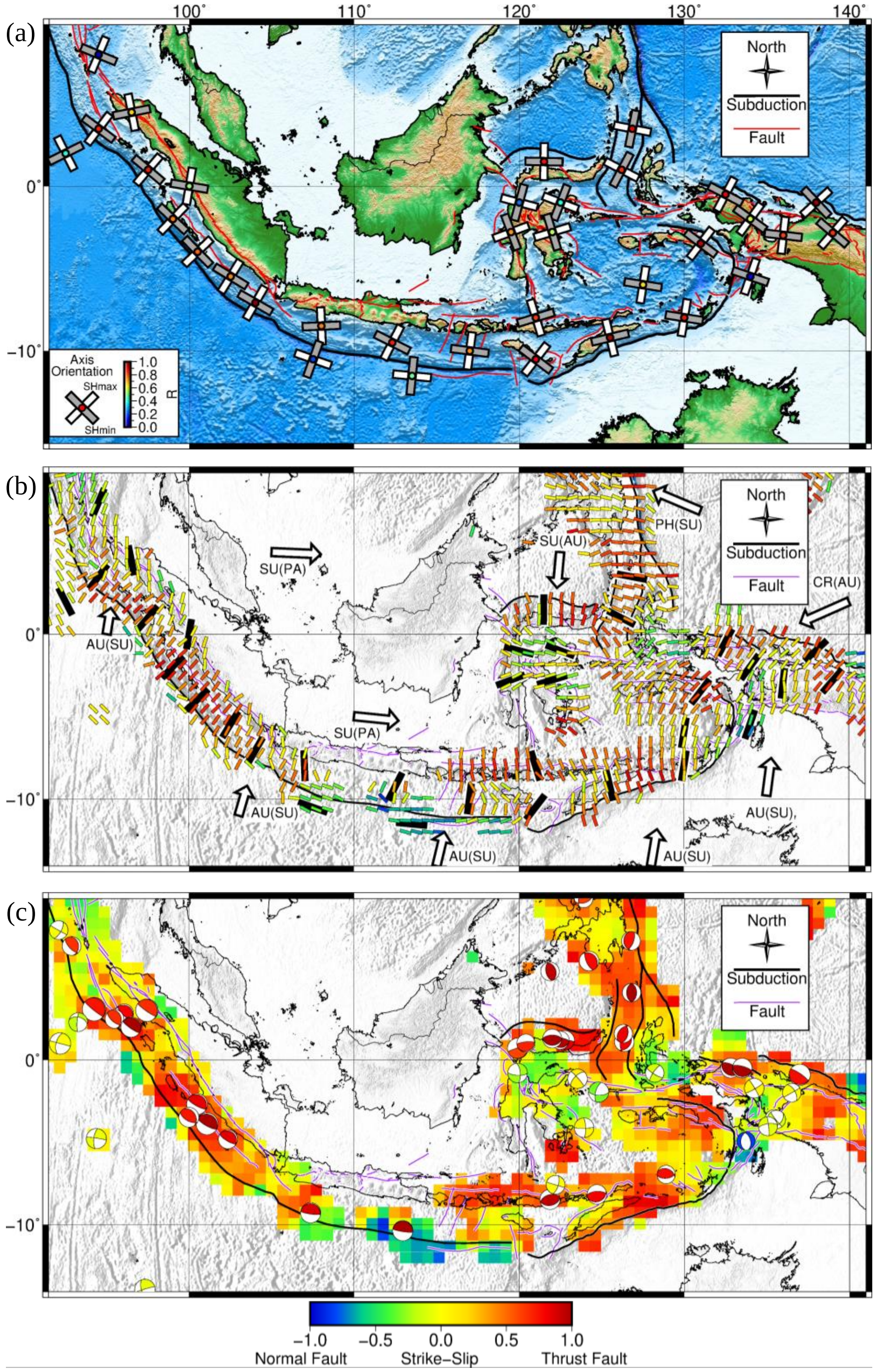

Figure 3. (a) Spatial distribution map of σ_1 and σ_3 azimuths of inversion result with stress ratio $R = (\sigma_1 - \sigma_2)/(\sigma_1 - \sigma_3)$. (b) SHmax comparison between two methodologies. (c) Comparison between spatial mean fault type with earthquake focal mechanism M≥7.

We confirmed that near the trench in Java and Sumba subduction segments, they are dominated by normal faults with the SHmax orientation which is parallel to the trench; in other words, the tensional stress directions are toward the trench, which is indicated as the uncouple subduction zone. This condition is consistent with results of stress tensor inversion, which revealed that the plunges of σ_1 in this area have relatively larger angles than other subduction segments. If the largest plunge is assumed as vertical stress and considering the stress ratio R value, it means that in this subduction regions, the tectonic stress regimes dominantly are indicated by pure to radial extensive in these segments (Delvaux et al., 1997). According to this study, our stress map provides the stress orientations and fault type mechanisms that can be used for evaluating seismicity in Indonesia. An advanced study can be done based on this stress map to evaluate the potential of fault slip.

ACKNOWLEDGEMENTS

This research was conducted during the individual study period of the training course “Seismology, Earthquake Engineering and Tsunami Disaster Mitigation” by the Building Research Institute, JICA, and GRIPS. I would like to express my sincere gratitude to Dr. Saeko Kita who has supervised and given me very useful guidance and advice that carried me through all the stages in this research project. I would also thank to Kazutoshi Imanishi and Makoto Ohtsubo from AIST for very nice discussion and suggestion about this research, Yo Fukushima from IRIDeS Tohoku University for his constructive comments, Václav Vavryčuk from Institute of Geophysics of the Czech Academy of Science and Björn Lund from Upssala University who have provided codes for stress inversion and SHmax calculation.

REFERENCES

Allmendinger, R. W., Reilinger, R., & Loveless, J., 2007, Tectonics, 26(3).
Bilek, S. L., & Engdahl, E. R., 2007, Geophysical Research Letters, 34(20).
Christensen, D. H., & Ruff, L. J., 1988, Journal of Geophysical Research: Solid Earth, 93(B11), 13421-13444.
Dziewonski, A. M., Chou, T.-A., & Woodhouse, J. H., 1981, Journal of Geophysical Research: Solid Earth, 86(B4), 2825-2852.
Ekström, G., Nettles, M., & Dziewoński, A. M., 2012, Physics of the Earth and Planetary Interiors, 200-201, 1-9.
Gephart, J. W., & Forsyth, D. W., 1984, Journal of Geophysical Research: Solid Earth, 89(B11), 9305-9320.
Heidbach, O., Tingay, M., Barth, A., Reinecker, J., Kurfeß, D., & Müller, B., 2010, Tectonophysics, 482(1), 3-15.
Imanishi, K., Uchide, T., Ohtani, M., Matsushita, R., Nakai, M., 2019, Bull. Geol. Surv. Japan, vol. 70 (3), p.273-298.
Inazu, D., Pulido, N., Fukuyama, E., Saito, T., Senda, J., & Kumagai, H., 2016, Earth, Planets and Space, 68(1), 73.
Irsyam, M., Widiyantoro, S., Natawidjaya, D. H., Meilano, I., Rudyanto, A., Hidayati, S., Triyoso, W., Hanifa, N. R., Djarwadi, D., Faizal, L., Sunarjito, 2017, Pusat Penelitian dan Pengembangan Perumahan dan Permukiman, Kementerian Pekerjaan Umum dan Perumahan Rakyat
Lentas, K, 2017, Geophysical Journal International, 212(3), 1665-1686.
Lentas, K., Di Giacomo, D., Harris, J., & Storchak, D. A., 2019, Earth Syst. Sci. Data, 11(2), 565-578.
Lund, B., & Slunga, R., 1999, Journal of Geophysical Research: Solid Earth, 104(B7), 14947-14964.
Lund, B., & Townend, J., 2007, Geophysical Journal International, 170(3), 1328-1335.
Mardia, K. V., 1972, Academic Press.
Michael, A. J., 1984, Journal of Geophysical Research: Solid Earth, 89(B13), 11517-11526.
Nakano, M., Yamashina, T., Kumagai, H., & Inoue, H., 2010, Physics of the Earth and Planetary Interiors, 183(3-4), 456-467.
Shearer, P. M., Prieto, G. A., & Hauksson, E., 2006, Journal of Geophysical Research: Solid Earth, 111(B6).
Vavryčuk, V., 2014, Geophysical Journal International, 199(1), 69-77.